JOURNAL OF MOLECULAR SPECTROSCOPY 107, 48–61 (1984)

Improved Deuterium Bromide 1-0 Band Molecular Constants from Heterodyne Frequency Measurements[1]

J. S. WELLS, D. A. JENNINGS

Time and Frequency Division, National Bureau of Standards, Boulder, Colorado 80303

AND

A. G. MAKI

Molecular Spectroscopy Division, National Bureau of Standards, Washington, D.C. 20234

Heterodyne frequency measurements have been made on selected deuterium bromide 1-0 band transitions ranging from $P(20)$ to $R(17)$. Difference frequency beat notes between a tunable-diode laser whose frequency was locked to the DBr absorption lines and a CO laser whose frequency was either locked or adjusted to a reference synthesized from CO_2 laser frequency standards were measured. The beat note frequency was then combined with the measured CO laser frequency to give the DBr frequency. For two of the measurements, frequency-doubled CO_2 laser radiation was substituted for the CO laser radiation. The measurements included electric quadrupole split triplets comprising the $R(0)$ and $P(1)$ transitions in the $D^{79}Br$ isotope. New DBr constants have been determined, and a table of frequencies is presented for the calibration of spectrometers and tunable lasers in the wavenumber range 1600 to 1990 cm^{-1}. A table of far-infrared frequencies is also given for DBr covering the range from 50 to 206 cm^{-1}.

INTRODUCTION

We have been engaged in an effort to provide a grid of calibrated molecular absorption frequency standards throughout the infrared region (*1–3*). Although carbonyl sulfide (OCS) provides excellent calibration standards in the region around 1710 cm^{-1} (*2, 3*) and around 1890 cm^{-1} (*3*), there are, nevertheless, several gaps in the region from 1600 to 2000 cm^{-1}. It has been suggested (*4, 5*) that the 1-0 band of deuterium bromide (DBr) may be useful for wavenumber (or frequency) calibration in that region. Although the presence of quadrupole fine structure and the wide spacing between absorption lines make this band rather unsuitable for certain calibration applications, the band has some advantages, particularly the large spectral coverage, that make it useful as an interim calibration standard.

The spectrum of the 1-0 band of DBr was first measured by Keller and Nielsen (*6*). Since then a number of improvements have been made in the measurements of the 1-0 band (*7–10*). Most recently Herman *et al.* (*10*) have reported very precise

[1] The authors wish to acknowledge the contributions by the late F. R. Petersen to the present work. It has been a privilege to work with Russ in the past; we miss his pleasant comaraderie, expertise in making difficult measurements, and meticulous attention to manuscripts. He will be sorely missed by the scientific community as a major contributor to the field of high-resolution spectroscopy.

0022-2852/84 $3.00

Fourier transform spectroscopy (FTS) measurements on the 1-0 band from $P(9)$ at 1757 cm^{-1} to $R(6)$ at 1894 cm^{-1}. They also reported the observation of laser Stark transitions for the $P(1)$ line of $D^{79}Br$.

Very accurate microwave measurements on the J = 1-0, 2-1, and 3-2 transitions in the ground vibrational state have been made for both $D^{81}Br$ and $D^{79}Br$ (*11, 12*). Van Dijk and Dymanus (*12*) have also measured the hyperfine coupling constants for both isotopic species in the ground vibrational state.

In this paper we report heterodyne frequency measurements on a number of rotational transitions in the v = 1-0 band of both $D^{81}Br$ and $D^{79}Br$. The measurements cover the wavenumber range from 1640 to 1961 cm^{-1}. These measurements are combined with some of the earlier measurements mentioned above to obtain a set of band constants and their uncertainties, which are used to calculate an improved list of frequencies and wavenumbers for use in the calibration of spectrometers and tunable laser devices.

EXPERIMENTAL TECHNIQUE

The basic procedure was as follows: A portion of the tunable-diode laser (TDL) radiation was used to lock the TDL frequency to that of a DBr absorption feature. The remaining part of the TDL radiation was heterodyned with radiation from a CO laser, which served as a transfer oscillator. The CO laser frequency was either locked or adjusted to a reference frequency which was synthesized from CO_2 laser frequency standards (*13, 14*). The TDL-CO laser frequency difference was then algebraically combined with the simultaneously measured CO laser frequency to give the DBr frequency.

DBr is a difficult molecule for this type of study. TDL coverage was a problem since only two lines 0.5 cm^{-1} apart appear at intervals ranging from 6 to 11 cm^{-1}, and the range of interest spans some 350 cm^{-1}. Additionally, the number of DBr-CO laser difference frequencies within our 5-GHz heterodyne range (limited by our spectrum analyzer) is not large, even considering the three CO isotopes available to use for CO laser operation.

As in previous experiments, the monochromator was adjusted to produce a zero-slope background either side of the line center to facilitate a first-derivative lock of the TDL frequency to the DBr absorption (*2, 15*). In cases where this was not practical, the lock was adjusted to compensate for any background slope. The 5-μm TDL had a larger jitter linewidth than was observed in some of our earlier work (*2, 15*). Since we estimate the uncertainty in the beat note center frequency to be one-tenth of the beat note linewidth, we avoid modulation which exceeds the jitter linewidth when possible. This has worked reasonably well for some of the stronger (0.5 mW) modes. Some TDLs used in this experiment exhibited wider linewidths at higher gain (proportional to the current) bandwidths. In order to find an optimal linewidth, we decreased the current (and increased the TDL cold mount temperature in order to maintain frequency) while we monitored the TDL linewidth. The optimal linewidth was the narrowest one attainable, provided that the reduced TDL power still gave a satisfactory S/N for the derivative lock. Half the frequency between the derivative

extrema divided by the S/N was taken as the other significant part of the frequency measurement uncertainty.

There were two reasons for using the CO laser as a transfer oscillator. First, the CO laser (at the fill pressure used (*16*)) does not lend itself to a satisfactory stabilization scheme, such as exists for the CO_2 laser (*17*). Second, our objective was to determine the DBr lines to within ±3 MHz, and our experience has indicated CO laser frequency tables in the literature are not always this accurate. In view of these considerations, we found it necessary to synthesize a reference frequency and then either lock or adjust the CO laser to this synthesized frequency. A block diagram of this scheme is indicated in Ref. (*2*). The apparatus for this synthesis included a MIM diode, two stabilized CO_2 lasers, and an X-band klystron. The radiation from the CO laser, the two CO_2 lasers, and the klystron all impinged on the MIM diode. The beat frequency, ν_B, which propagated from the MIM diode, was equal to

$$\nu_B = \nu_{CO} - (l\nu_1 + m\nu_2 + n\nu_{\mu w})$$

where ν_{CO}, ν_1, ν_2 and $\nu_{\mu w}$ are the frequencies of the CO laser, a $^{13}C^{16}O_2$ laser, a $^{12}C^{16}O_2$ laser, and an X-band klystron, respectively. The harmonic numbers, l, m, and n can be either positive or negative integers. The beat signal, typically on the order of 100 MHz, was amplified and displayed on a spectrum analyzer. The CO laser was tuned to the midpoint between the two frequencies, marking the disappearance of the beat signal as the CO laser was tuned across its gain bandwidth. Thus, the measurement is also a determination of the CO laser line frequency. We estimate that the CO line center could be determined to within ±3 MHz. It should be emphasized, however, that the accuracy of the DBr measurement does not depend on locating the center of the CO lines, since the CO laser frequency was either manually adjusted or locked to a synthesized frequency while the TDL-CO laser frequency differences were measured. This last (and least) contribution to the DBr frequency uncertainty was less than 0.2 MHz.

We note that the CO frequency values in the literature could be as much as 20–30 MHz different from our measured values; hence, our measurements were essential to achieving our objective of obtaining an accuracy of ±3 MHz for the DBr frequencies.

The DBr absorption cell was 1.7 m long, and the DBr pressures varied between 0.01 and 0.33 kPa (0.1 to 2.5 Torr). The measured DBr frequencies are listed in Table I, along with the species and transitions used for the CO lasers operating in the transfer oscillator mode. One $^{12}C^{18}O$, five $^{13}C^{16}O$, and five $^{12}C^{16}O$ laser transitions were used in these measurements. Typical CO laser operating pressures were 2.40 to 2.66 kPa (18 to 20 Torr) total pressure. For $^{12}C^{16}O$, volume percentages were 6.3% each for CO, N_2, and Xe, and the balance was He. For $^{13}C^{16}O$ and $^{12}C^{18}O$ operation (and also for $P_{18}(11)$ of $^{12}C^{16}O$) an additional 6.3% CO was substituted for N_2. The measured CO laser frequencies are also given in Table I.

Also listed in Table I are two measurements in which doubled CO_2 laser radiation was substituted for CO laser radiation. We believe this is the first reported measurement of this type. Approximately 6 W CO_2 laser radiation was focused by a 60-mm lens into a $CdGeAs_2$ nonlinear crystal which was cooled in a nitrogen dewar. This crystal is more than an order of magnitude more efficient than Te as a frequency doubler at 10 μm (*18, 19*). Phase matching was achieved by angle tuning and the sub-mW

level power was collimated by a 125-mm Ge lens. (The transmitted pump beam was blocked by a sapphire window.) In previous CO and CO_2 laser heterodyne experiments a NaCl beam splitter at 45° to the radiation direction was used, and the laser radiation was coupled to the HgCdTe heterodyne detector in the TM polarization, resulting in about 0.8% coupling. The doubled CO_2 radiation emerged from the crystal with polarization perpendicular to the CO_2 pump beam; thus, a ZnSe beam splitter and coupling in the TE polarization permitted about 30% coupling to the heterodyne detector. This was sufficient to observe a good beat note at 233 MHz for one measurement and a barely usable beat note at 1290 MHz for the other. (The highest frequency beat note observed in these measurements with the CO laser was 4444 MHz.)

ANALYSIS OF THE MEASUREMENTS

Analysis of the Quadrupole Fine Structure

The results of these measurements are given in Table I. The $P(1)$ and $R(0)$ transitions quite clearly showed the three fine-structure components due to the coupling of the quadrupole moment of the bromine atom with the rotational angular momentum of the molecule (see Fig. 1). For the $P(1)$ transition the quadrupole splitting is in the

TABLE I

Heterodyne Frequency Measurements on the 1-0 Band of Both Isotopes of Deuterium Bromide

Deuterium Bromide				Transfer Laser		
Species	Transition	Measured Freq. (MHz)	Obs-calc. (MHz)	Species	Trans.	CO Ref. Freq. (MHz)
$D^{79}Br$	P(20)	49 202 938.2(100)[a]	3.8	$^{13}C^{16}O$	$P_{16}(17)$	49 205 269.23[b]
	P(9)	52 699 156.4(80)	0.0	$^{12}C^{18}O$	$P_{11}(17)$	52 699 015.64
	P(6)	53 563 244.3(70)	-0.2	$^{13}C^{16}O$	$P_{11}(10)$	53 561 840.55
	P(1),F=3/2←3/2	54 909 742.6(60)	1.7	$^{13}C^{16}O$	$P_9(11)$	54 910 365.32
	P(1),F=3/2←5/2	54 909 875.0(60)	1.8	$^{13}C^{16}O$	$P_9(11)$	54 910 365.32
	R(0),F=5/2←3/2	55 414 205.4(60)	-1.6	$^{13}C^{16}O$	$P_8(13)$	55 415 775.44
	R(0),F=3/2←3/2	55 414 345.3(60)	-1.6	$^{13}C^{16}O$	$P_8(13)$	55 415 775.44
	R(3)	56 132 526.8(100)	0.4	$^{12}C^{16}O$	$P_8(16)$	56 128 082.85
	R(15)	58 515 084.3(50)	-0.5	$^{12}C^{16}O_2$	$R_1(20)$	c
$D^{81}Br$	P(20)	49 190 291.5(60)	1.1	$^{12}C^{16}O$	$P_{18}(11)$	49 187 920.76
	P(7)	53 264 416.6(180)	2.3	$^{13}C^{16}O$	$P_{10}(19)$	53 267 366.6[d]
	P(3)	54 369 576.7(80)	-2.6	$^{12}C^{16}O$	$P_{10}(18)$	54 367 877.99
	R(2)	55 881 317.6(80)	1.8	$^{12}C^{16}O$	$P_8(18)$	55 880 994.66
	R(9)	57 407 326.0(100)	2.7	$^{12}C^{16}O$	$P_6(18)$	57 403 403.61
	R(17)	58 812 745.6(150)	-12.6	$^{12}C^{16}O_2$	$R_1(28)$	c

a) The estimated uncertainties (2 σ) in the last digits are given in parentheses.
b) The estimated uncertainty (2 σ) in determining the absolute frequency of the CO laser line center is ± 3 MHz.
c) The doubled frequency of this CO_2 laser transition was the reference frequency for this measurement.
d) The line center was not determined for this laser transition.

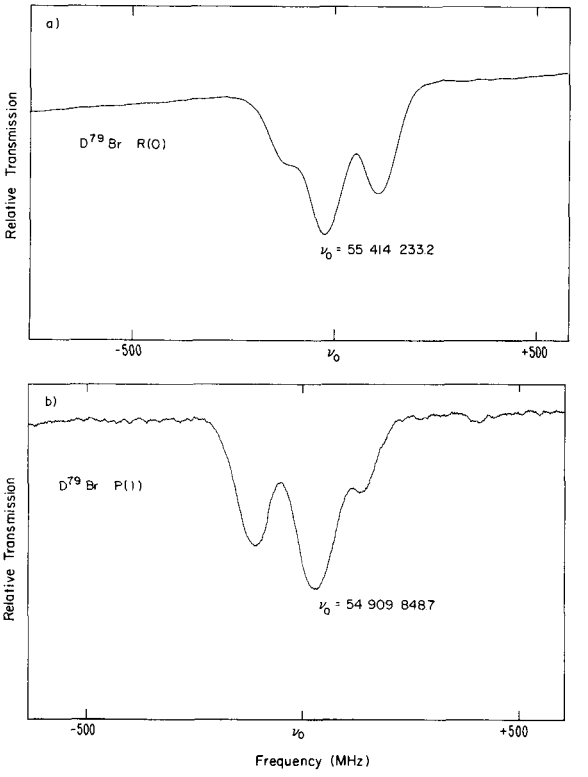

FIG. 1. Absorption spectra which exhibit quadrupole splitting are shown for (a) $R(0)$ and (b) $P(1)$ of $D^{79}Br$. The tic at ν_0 represents the center of gravity of each triplet. The spectra were recorded at a pressure of 25 Pa and a path length of 1.7 m. Signal-to-noise and tuning rates differ due to the use of different diode lasers for the two transitions.

ground vibrational, state whereas for the $R(0)$ transition the splitting is in the $v = 1$ state. Van Dijk and Dymanus (*12*) have given quite accurate values for the coupling constants in the ground vibrational state, and we have used their values to determine the hypothetical unsplit $P(1)$ line position (ν_0 in Fig. 1b) The hypothetical unsplit line positions were used in the determination of the band constants. Since no previous measurements have given the quadrupole coupling for the upper vibrational state, we have used the observed splitting of the $R(0)$ transition to obtain a value for the upper state coupling constant eqQ. All of the coupling constants used in this analysis are given in Table II.

A first step in the analysis of the $P(1)$ and $R(0)$ transitions was to make a small correction for the shifts in the apparent absorption maxima due to the overlap of adjacent quadrupole transitions. This correction was made by measuring the shifts in the absorption maxima of $P(1)$ for a calculated spectrum made by using the splitting given by the microwave measurements and a linewidth adjusted to match the observed spectrum. The corrections used for the $R(0)$ transitions were +0.2 MHz for the strongest transition ($F = 5/2 \leftarrow 3/2$), +1.2 MHz for the weaker $F = 3/2 \leftarrow 3/2$, and

TABLE II

Hyperfine Coupling Constants (in MHz) for DBr

	$D^{79}Br$	$D^{81}Br$
eqQ(v=0)	530.631[a]	443.280[a]
C_{Br}(v=0)	0.146[a]	0.157[a]
eqQ(v=1)	557.2±10.0	
C_{Br}(v=1)	0.146[b]	

a) Values taken from Ref. 12.

b) The value of C_{Br} was assumed to be the same in both v=0 and v=1.

−7 MHz for the weakest transition ($F = 1/2 \leftarrow 3/2$). The corrections were the same, but reversed in sign, for the equivalent $P(1)$ transitions. Since the weakest transition was shifted the greatest amount and since it was also the most sensitive to small variations in the effective spectral resolution, the measurements of those transitions were not used in the analysis and are not reported in Table I.

We have fit the present DBr measurements in two stages. The first stage involved a global fit of all the DBr infrared and microwave measurements to obtain the best set of centrifugal distortion constants from the Dunham potential constants. The second stage involved a fit in which the present data, and data from three other papers (*10–12*), were fit to obtain the best values for the 1-0 band center and rotational constants for each isotopic species. In the next two sections these two stages will be justified and described in the order in which they were carried out.

The Global Fit

The traditional way of fitting data on a single vibrational transition uses the rotational energy level equation

$$F(v, J) = B_v J(J+1) - D_v J^2(J+1)^2 + H_v J^3(J+1)^3 + L_v J^4(J+1)^4 + S_v J^5(J+1)^5, \quad (1)$$

and the transition frequency equation

$$\nu_{obs} = \nu_0 + F(v', J') - F(v'', J''), \quad (2)$$

where the $'$ and $''$ indicate upper and lower state quantum numbers, respectively. If pure rotational transitions are involved, as for the microwave transitions, then $\nu_0 = 0$ and $v' = v''$.

Dunham (*20*) has shown that for diatomic molecules the ν_0, B_v, D_v, H_v, etc. terms can be related to a set of molecular constants, Y_{ij}, such that

$$G(v, J) = \Sigma_{ij} Y_{ij} \left(v + \frac{1}{2}\right)^i [J(J+1)]^j \quad (3)$$

and

$$\nu_{obs} = G' - G''. \tag{4}$$

Dunham also showed that the Y_{ij} constants can be related to a potential function containing the Dunham potential constants ω_e, B_e, a_1, a_2, a_3 $\cdots$ etc.

Most workers in the past have fit the measured transitions to the Y_{ij} constants and then calculated the potential constants from the Y_{ij} constants. Niay *et al.* (*21*) have done the opposite. They have used a nonlinear least-squares technique to fit the observed transitions of HBr directly to a set of Dunham potential constants, and then they have used the potential constants to calculate the Y_{ij} constants. Maki and Lovas have used a similar technique to fit the spectrum of several diatomic species including SnO (*22*), KF and AlF (*23*), and the two isotopic species of LiF (*24*).

Fitting the data directly to the Dunham potential constants takes advantage of the connection between the centrifugal distortion constants and the vibrational anharmonicity constants that is implicit in our understanding of the potential function and energy levels for a diatomic molecule. The traditional way of fitting the transitions to Eqs. (1) and (2), or equivalently to Eqs. (3) and (4), is often unable to determine the centrifugal distortion constants very well. This traditional technique is also likely to produce large errors when the constants are used to extrapolate to unmeasured transitions.

Since the goal of this paper is to present the most accurate possible table of calculated frequencies for the 1-0 transitions of DBr, we have determined the centrifugal distortion constants for this band from a global fit of all the microwave (*11, 12*) and infrared (*8, 10, 25*) transitions that are available to us. Table III indicates what data were used in this global fit and the uncertainties used to weight each data set. This fit used the nonlinear least-squares program used in Refs. (*22–24*) that fits the transitions directly to a set of potential constants, and then uses the potential constants to obtain a set of Y_{ij} constants and their uncertainties.

TABLE III

Summary of the Data Used to Calculate the Dunham Potential Constants for DBr

Vibrational Transition	J_{max}	Absolute Uncertainty (MHz)	No. of Data	Ref.
0-0	1	0.0004	2	12
0-0	3	0.1-0.3	12	11
1-0	20	see Table I	17	present work
1-0	8	8	18	10
1-0	37	400	24[a]	8
2-0	24	300	89	8
3-0	16	100	53	8
4-0	12	100	41	8
5-0	12	800	39	25

a) Only the measurements for R(24) to R(36) were used for the 1-0 band from Ref. (8).

As a first approximation the same potential constants can be applied to any isotopic species of the same molecule by using the mass reduced constants U_B and U_ω defined as

$$B_e = U_B \mu^{-1} \tag{5}$$

and

$$\omega_e = U_\omega \mu^{-1/2}, \tag{6}$$

where μ is the reduced mass of the molecule. This was satisfactory for treating the several isotopes of tin in SnO (*22*), but it fails for the light atoms such as the lithium isotopes in LiF (*24*), and even for certain heavy atoms such as the lead isotopes in PbS (*26*).

Bunker (*27*) and Watson (*28*) have shown that the mass dependence of the Dunham constants can be accurately given by

$$Y_{ij} = U_{ij} \mu^{-(i+2j)/2} \left[1 + \frac{m_e}{m_a} \Delta_{ij}^a + \frac{m_e}{m_b} \Delta_{ij}^b \right], \tag{7}$$

where U_{ij} is a mass reduced constant, μ is the reduced mass for the ab molecule, m_e is the mass of an electron, m_a is the mass of atom a, and m_b is the mass of atom b. Normally the Δ_{ij} terms have values close to or smaller than 1.

By analogy with Eq. (7), and because $Y_{01} \sim B_e$ and $Y_{10} \sim \omega_e$, we have used the equations

$$B_e = U_e \mu^{-1} \left[1 + \frac{m_e}{m_a} \Delta_B^a + \frac{m_e}{m_b} \Delta_B^b \right] \tag{8}$$

and

$$\omega_e = U_\omega \mu^{-1/2} \left[1 + \frac{m_e}{m_a} \Delta_\omega^a + \frac{m_e}{m_b} \Delta_\omega^b \right] \tag{9}$$

rather than Eqs. (5) and (6). With Eqs. (8) and (9) the two isotopes of LiF (*24*) and several isotopes of PbS (*26*) have been fit to a single set of Dunham potential constants so we have confidence that this can also be done for the two bromine isotopes in DBr. In the present calculations the following masses were used (*29, 30*):

$$m(^{79}\text{Br}) = 78.9183361\ u$$

$$m(^{81}\text{Br}) = 80.916290\ u$$

$$m(\text{D}) = 2.014101787\ u$$

and

$$m_e = 5.4858026 \times 10^{-4}\ u.$$

In summary, the global fit used the data for both bromine isotopes indicated in Table III, weighted by the inverse square of the estimated uncertainty, in a nonlinear least-squares fit to obtain the Dunham potential constants given in Table IV. In this fit we used Eqs. (8) and (9) and the equations given by Dunham (*20*), and Bouanich (*31*). Equations involving constants higher than a_6 were not used. These potential constants were used to calculate the Y_{ij} constants given in Table V. These Y_{ij} constants were, in turn, used to calculate the centrifugal distortion and higher order terms given

TABLE IV

Dunham Potential Constants Determined for DBr

B_e ($D^{79}Br$)(MHz)	128 538.6587(238)[a]
ω_e ($D^{79}Br$)(MHz)	56 527 934.3(630)
B_e ($D^{81}Br$)(MHz)	128 538.6612(238)
ω_e ($D^{81}Br$)(MHz)	56 527 931.7(630)
U_B (MHz·u)	252 602.5661(478)
Δ_B^{Br}	-0.11074(587)[b]
U_ω (MHz·$u^{\frac{1}{2}}$)	79 243 593.1(1262)
Δ_ω^{Br}	0.2604(1549)
a_1	-2.435 543 37(6992)[b]
a_2	3.831 169 2(3862)
a_3	-5.039 079(3828)
a_4	5.862 85(3239)
a_5	-7.015 0(1109)
a_6	11.430 8(2593)

a) The estimated standard error in the last digits is given in parentheses.

b) The Δ's and a_i's are dimensionless quantities.

TABLE V

Dunham Coefficients for DBr

	$D^{81}Br$	$D^{79}Br$
Y_{10}(MHz)	56 526 955.65(6131)[a]	56 544 332.96(6122)[a]
Y_{20}(MHz)	-690 985.92(5151)	-691 410.78(5151)
Y_{30}(MHz)	1 086.90(1514)	1 087.90(1514)
Y_{40}(MHz)	-98.920(1447)	-99.041(1447)
Y_{01}(MHz)	128 537.343 84(4407)	128 616.372 92(4407)
Y_{11}(MHz)	-2 517.805 0(1283)	-2 520.1274(1283)
Y_{21}(MHz)	5.552 7(877)	5.5595(877)
Y_{31}(MHz)	-0.524 97(1461)	-0.525 77(1461)
Y_{02}(MHz)	-2.658 559 11(701)	-2.661 829 04(701)
Y_{12}(kHz)	19.080 45(2076)	19.109 80(2076)
Y_{22}(Hz)	-753.79 (1630)	-755.18(1630)
Y_{32}(Hz)	-51.667(3155)	-51.778(3155)
Y_{03}(Hz)	31.021 37(408)	31.078 61(408)
Y_{13}(Hz)	-0.803 08(1058)	-0.804 81(1058)
Y_{23}(mHz)	-90.392 (2799)	-90.614(2799)
Y_{04}(mHz)	-0.677 376(331)	-0.679 043(331)
Y_{14}(μHz)	-22.693 (1434)	-22.756 (1434)
Y_{05}(nHz)	6.934 3(951)	6.955 6(951)

a) The estimated standard error in the last digits is given in parentheses.

in Table VI, but not the values of ν_0, B_0, and B_1 which were determined as described in the next section.

Fit of the Data for the 1-0 Band

The present measurements, the microwave measurements, and the very good FTS measurements of Herman *et al.* (*10*) were used to determine the values of ν_0, B_0, and B_1. The FTS data were allowed to determine a different ν_0 (which was not used to calculate the frequencies in Table VII) because they seem to have a small systematic calibration error. A separate least-squares fit was made for each isotopic species by using Eqs. (1) and (2). The centrifugal and higher-order terms were fixed at the values determined by the global fit just described and given in Table VI.

There are two reasons why we did not use the values of ν_0, B_0, and B_1 given by the potential constants. First, these are the constants that can be determined with the most significant figures and we were not certain that Eqs. (8) and (9) are sufficiently accurate. Second, some of the data used to determine the potential constants may have systematic calibration errors. For instance, some measurements used DBr at a pressure of 9.3 kPa (70 Torr) or greater and undoubtedly have systematic pressure shifts. We believe these systematic errors will have no significant effect on the centrifugal distortion terms, but may affect the terms that have the most significant figures.

The constants given in Table VI were used to calculate the frequencies given in Tables VII and VIII. The uncertainties given in Tables VII and VIII were calculated using the variance–covariance matrix for the Y_{ij} constants given in Table V. We believe this is the best way to estimate the uncertainties in the calculated transitions even though the values of ν_0, B_0, and B_2 were not taken from Table V.

TABLE VI

Constants for DBr Used to Calculate the Transitions in Tables VII and VIII

	$D^{81}Br$	$D^{79}Br$
ν_0(MHz)	55 148 021.66(211)[a]	55 164 551.528(973)[a]
B_1(MHz)	124 771.360 12(852)	124 846.919 38(580)
D_1(kHz)	2 631.808 833(5190)	2 635.038 249(5192)
H_1(Hz)	29.613 364(6342)	29.667 508(6343)
L_1(μHz)	-711.416(1880)	-713.178 (1880)
S_1(nHz)	6.934 3(951)	6.955 6(951)
B_0(MHz)	127 279.763 906(82)	127 357.633 366(87)
D_0(kHz)	2 649.213 788(363)	2 652.469 411(330)
H_0(Hz)	30.597 230(631)	30.653 549(631)
L_0(μHz)	-688.723(471)	-690.422 (471)
S_0(nHz)	6.934 3(951)	6.955 6(951)

a) The estimated standard error in the last digits is given in parentheses.

TABLE VII

Frequencies and Wavenumbers[a] of the V = 1-0 Transitions of DBr

	$D^{81}Br$		$D^{79}Br$	
TRANSITION	FREQUENCY (MHz)	WAVENUMBER[a] (cm^{-1})	FREQUENCY (MHz)	WAVENUMBER (cm^{-1})
P(24)	47804143.3(77)[b]	1594.57458(26)	47815845.2(82)	1594.96491(27)
P(23)	48155995.8(71)	1606.31112(24)	48167937.5(75)	1606.70945(25)
P(22)	48504348.7(65)	1617.93092(22)	48516527.3(68)	1618.33715(23)
P(21)	48849135.6(60)	1629.43177(20)	48861548.4(62)	1629.84582(21)
P(20)	49190290.4(56)	1640.81147(19)	49202934.4(56)	1641.23323(19)
P(19)	49527746.4(52)	1652.06779(17)	49540618.6(51)	1652.49716(17)
P(18)	49861436.9(48)	1663.19851(16)	49874534.3(46)	1663.63539(15)
P(17)	50191295.3(45)	1674.20140(15)	50204614.6(41)	1674.64568(14)
P(16)	50517254.6(43)	1685.07423(14)	50530792.7(37)	1685.52581(12)
P(15)	50839248.1(42)	1695.81478(14)	50853001.5(34)	1696.27354(11)
P(14)	51157208.8(41)	1706.42081(14)	51171174.3(31)	1706.88664(10)
P(13)	51471070.0(40)	1716.89009(14)	51485244.0(29)	1717.362881(97)
P(12)	51780764.8(41)	1727.22040(14)	51795143.7(28)	1727.700025(92)
P(11)	52086226.6(41)	1737.40950(14)	52100806.8(27)	1737.895848(89)
P(10)	52387388.8(42)	1747.45519(14)	52402166.6(26)	1747.948127(88)
P(9)	52684184.9(42)	1757.35525(14)	52699156.4(26)	1757.854643(88)
P(8)	52976548.8(43)	1767.10746(14)	52991710.1(27)	1767.613184(89)
P(7)	53264414.3(44)	1776.70961(15)	53279761.4(27)	1777.221541(91)
P(6)	53547715.5(45)	1786.15953(15)	53563244.5(28)	1786.677517(93)
P(5)	53826386.9(46)	1795.45500(15)	53842093.5(29)	1795.978921(95)
P(4)	54100363.2(47)	1804.59387(15)	54116243.2(29)	1805.123571(97)
P(3)	54369579.3(47)	1813.57395(16)	54385628.5(30)	1814.109296(99)
P(2)	54633970.6(47)	1822.39310(16)	54650184.5(30)	1822.93394(10)
P(1)	54893472.7(48)	1831.04916(16)	54909846.9(30)	1831.59534(10)
R(0)	55397553.9(47)	1847.86349(16)	55414234.8(30)	1848.41991(10)
R(1)	55642006.2(47)	1856.01754(16)	55658833.5(30)	1856.578845(99)
R(2)	55881315.8(47)	1864.00006(16)	55898284.8(29)	1864.566081(97)
R(3)	56115420.6(46)	1871.80895(15)	56132526.4(29)	1872.379539(95)
R(4)	56344258.8(45)	1879.44217(15)	56361496.5(28)	1880.017157(93)
R(5)	56567769.0(44)	1886.89767(15)	56585133.5(27)	1887.476887(91)
R(6)	56785890.5(43)	1894.17342(14)	56803376.8(27)	1894.756699(89)
R(7)	56998563.1(43)	1901.26741(14)	57016166.0(26)	1901.854584(88)
R(8)	57205727.1(42)	1908.17766(14)	57223441.4(26)	1908.768546(88)
R(9)	57407323.3(41)	1914.90219(14)	57425143.8(27)	1915.496613(89)
R(10)	57603293.3(41)	1921.43904(14)	57621214.5(28)	1922.036828(92)
R(11)	57793579.0(41)	1927.78629(14)	57811595.6(29)	1928.387258(97)
R(12)	57978123.3(41)	1933.94202(14)	57996229.6(31)	1934.54599(10)
R(13)	58156869.2(42)	1939.90435(14)	58175059.9(34)	1940.51112(11)
R(14)	58329760.8(43)	1945.67139(14)	58348030.1(37)	1946.28079(12)
R(15)	58496742.6(45)	1951.24130(15)	58515084.8(41)	1951.85313(14)
R(16)	58657759.8(48)	1956.61226(16)	58676169.2(46)	1957.22633(15)
R(17)	58812758.2(52)	1961.78245(17)	58831228.9(51)	1962.39856(17)
R(18)	58961684.3(56)	1966.75009(19)	58980210.5(56)	1967.36805(19)
R(19)	59104485.3(60)	1971.51342(20)	59123061.0(62)	1972.13304(21)
R(20)	59241109.1(65)	1976.07070(22)	59259728.3(68)	1976.69176(23)
R(21)	59371504.1(71)	1980.42020(24)	59390160.7(75)	1981.04252(25)
R(22)	59495619.4(77)	1984.56025(26)	59514307.4(81)	1985.18361(27)
R(23)	59613405.0(83)	1988.48915(28)	59632118.0(89)	1989.11335(30)
R(24)	59724811.2(90)	1992.20526(30)	59743543.1(96)	1992.83009(32)

[a]The frequency values have been converted to wavenumbers by using c=299792.458 km/s.

[b]The uncertainty in the last digits (three times the standard error) is given in parentheses.

After this analysis was completed, we found that the values of ν_0, B_0, and B_1 as determined from the global fit were in agreement with the values given in Table VI to within a small fraction of the standard error.

TABLE VIII

Frequencies and Wavenumbers[a] of the Rotational Far-Infrared Transitions of DBr

	$D^{81}Br$		$D^{79}Br$	
TRANSITION J' - J"	FREQUENCY (MHz)	WAVENUMBER[a] (cm^{-1})	FREQUENCY (MHz)	WAVENUMBER (cm^{-1})
6 - 5	1525069.685(3)[b]	50.87084897(11)	1526001.309(3)	50.90192458(11)
7 - 6	1778285.075(4)	59.31720521(13)	1779370.787(4)	59.35342065(13)
8 - 7	2031056.668(5)	67.74875797(15)	2032295.923(5)	67.79009507(15)
9 - 8	2283321.501(5)	76.16340706(18)	2284713.678(5)	76.20984508(17)
10 - 9	2535016.787(6)	84.55905808(21)	2536561.187(6)	84.61057374(20)
11 - 10	2786079.931(7)	92.93362315(24)	2787775.781(7)	92.99019060(23)
12 - 11	3036448.557(8)	101.28502155(28)	3038295.005(8)	101.34661242(26)
13 - 12	3286060.521(9)	109.61118046(32)	3288056.642(9)	109.67776387(29)
14 - 13	3534853.940(11)	117.91003561(36)	3536998.732(10)	117.98157817(33)
15 - 14	3782767.203(12)	126.17953195(40)	3785059.591(11)	126.25599777(36)
16 - 15	4029738.998(14)	134.41762428(45)	4032177.832(12)	134.49897501(39)
17 - 16	4275708.326(15)	142.62227790(50)	4278292.383(13)	142.70847276(43)
18 - 17	4520614.522(17)	150.79146927(56)	4523342.506(14)	150.88246503(46)
19 - 18	4764397.273(18)	158.92318656(61)	4767267.817(15)	159.01893758(50)
20 - 19	5006996.637(20)	167.01543029(67)	5010008.300(16)	167.11588856(53)
21 - 20	5248353.057(22)	175.06621389(73)	5251504.330(17)	175.17132904(56)
22 - 21	5488407.383(24)	183.07356429(79)	5491696.685(18)	183.18328358(59)
23 - 22	5727100.883(26)	191.03552242(85)	5730526.564(19)	191.14979084(62)
24 - 23	5964375.263(27)	198.95014379(92)	5967935.604(20)	199.06890400(66)
25 - 24	6200172.679(29)	206.81549896(98)	6203865.895(21)	206.93869139(69)

[a]The frequency values have been converted to wavenumbers by using c=299792.458 km/s.

[b]The uncertainty in the last digits (three times the standard error) is given in parentheses.

DISCUSSION

The frequencies given in Tables VII and VIII were calculated without allowing for the quadrupole splitting of the energy levels. For transitions involving $J > 5$ the quadrupole splitting, when barely resolved, will give rise to two distinct absorption features, one stronger than the other. The separation of this doublet will vary from about 6 MHz for $J = 5$ to 2 MHz or less for $J \geqslant 10$. If DBr is measured by a technique for which the resolution is approaching the separation of the quadrupole features, the line profile may be distorted and the apparent line center may deviate from the frequency given in the tables. This effect, however, will always be smaller than the separation of the quadrupole doublet features. The frequencies given in Tables VII and VIII represent the center of gravity of all the quadrupole transitions and do not designate the precise mid-point between the two distinct quadrupole features just mentioned.

A major concern in using any gas for calibration at the level of accuracy we are approaching is the pressure induced shift of the absorption frequencies. A crude attempt at measuring the pressure shift of the $P(20)$ line of $D^{81}Br$ gave a value of -5.3 ± 7.5 MHz/kPa (-0.7 ± 1.0 MHz/Torr). We know of no other measurement of the pressure shift of DBr by DBr for infrared rovibrational transitions. Since our measurements were made at less than 0.400 kPa (3 Torr), the error due to the pressure

shift is probably no greater than the other sources of experimental error, but a careful study of the pressure shift of DBr should be made.

The wavenumbers given in Table VII are in excellent agreement with previous listings (*5, 9*). The wavenumbers given by Cole and Cugley are consistently high but by less than 0.001 cm^{-1}, which is within their ± 0.002 cm^{-1} error limit. The band centers are within 0.002 cm^{-1} of the band centers given by Fayt *et al.* (*8*). Our reanalysis of the data of Herman *et al.* (*10*) gives nearly the same band centers as their analysis, but our measurements indicate that their measurements are too high by about 17 MHz, which is about the absolute uncertainty that they gave. On the other hand, the calculated value of the $P(1)$ transition of $D^{79}Br$, given in Table VII, is only 4 MHz lower than the laser Stark measurement of Herman *et al.*

The Dunham potential constants given in Table III are within two standard deviations of the values given by Bernage and Niay (*25*), although they only determined values through a_4. The Y_{ij} constants are not as close to the values given by Bernage and Niay or those given by Fayt *et al.* (*8*), some disagreements being four or more times their standard deviation. We attribute this difference to the more extensive data set that we are using.

Guelachvili *et al.* (*32*) have recently published a set of Dunham constants which we have used to calculate the CO laser transition frequencies to see how well the calculated frequencies agree with the present measurements. The calculated frequencies are all too high by 5 to 10 MHz, with the exception of the $^{13}C^{16}O$ $P_{11}(10)$ transition which is 1 MHz less than the measured value. This disagreement is probably due to a small systematic error in most of the CO measurements used in Ref. (*32*). If the values of Y_{10} for all isotopes of CO were lowered by 5 or 6 MHz, the agreement with our measurements would be much better.

We have also compared the present measurements with the tables of CO laser wavenumbers given by Dale *et al.* (*33*). We find excellent agreement for laser transitions at frequencies greater than 54 THz; in fact, the agreement is better than for the constants given by Guelachvili *et al.* At lower frequencies, the tables of Dale *et al.* seem to get progressively worse, the values being too small by 25 to 30 MHz at 49 THz.

ACKNOWLEDGMENTS

This work was supported in part by the Upper Atmospheric Research Division of NASA. We would like to thank N. Menyuk, G. W. Iseler, and A. Mooradian of MIT for the use of their frequency-doubling crystal. We are also grateful to Laser Analytics Division of Spectra Physics for their cooperation in providing a large number of lasers for purchasing consideration.

RECEIVED: March 30, 1984

REFERENCES

1. C. R. POLLOCK, F. R. PETERSEN, D. A. JENNINGS, J. S. WELLS, AND A. G. MAKI, *J. Mol. Spectrosc.* **99**, 357–368 (1983).
2. J. S. WELLS, F. R. PETERSEN, AND A. G. MAKI, *J. Mol. Spectrosc.* **98**, 404–412 (1983).
3. A. G. MAKI, J. S. WELLS, F. R. PETERSEN, W. B. OLSON, A. FAYT, AND J. P. SATTLER, *J. Phys. Chem. Ref. Data,* in press.

4. H. W. THOMPSON, "Tables of Wavenumbers for the Calibration of Infrared Spectrometers" (first edition prepared by the Commission on Molecular Structure and Spectroscopy of IUPAC) Reprinted from *Pure Appl.Chem.* **1** (1961) (Butterworths, London, 1961).
5. A. R. H. COLE, "Tables of Wavenumbers for the Calibration of Infrared Spectrometers," 2nd ed., Pergamon, Oxford, 1977.
6. F. L. KELLER AND A. H. NIELSEN, *J. Chem. Phys.* **22,** 294–299 (1954).
7. H. M. MOULD, W. C. PRICE, AND G. R. WILKINSON, *Spectrochim. Acta* **16,** 479–492 (1960).
8. A. FAYT, D. VAN LERBERGHE, G. GUELACHVILI, C. AMIOT, P. BERNAGE, AND P. NIAY, *Mol. Phys.* **32,** 955–962 (1976).
9. A. R. H. COLE AND J. A. CUGLEY, *Indian J. Pure Appl. Phys.* **16,** 419–421 (1978).
10. M. HERMAN, J. W. C. JOHNS, AND A. R. W. MCKELLAR, *J. Mol. Spectrosc.* **95,** 405–412 (1982).
11. F. C. DELUCIA, P. HELMINGER, AND W. GORDY, *Phys. Rev. A* **3,** 1849–1857 (1971).
12. F. A. VAN DIJK AND A. DYMANUS, *Chem. Phys.* **6,** 474–478 (1974).
13. C. FREED, L. C. BRADLEY, AND R. G. O'DONNELL, *IEEE J. Quant. Elect.* **16,** 1195–1206 (1980).
14. F. R. PETERSEN, E. C. BEATY, AND C. R. POLLOCK, *J. Mol. Spectrosc.* **102,** 112–122 (1983).
15. J. S. WELLS, F. R. PETERSEN, AND A. G. MAKI, *Appl. Opt.* **18,** 3567–3573 (1979).
16. C. FREED AND H. A. HAUS, *IEEE J. Quant. Elect.* **QE-9,** 219–226 (1973).
17. C. FREED AND A. JAVAN, *Appl. Phys. Lett.* **17,** 53–56 (1970).
18. R. L. BYER, H. KILDAL, AND R. S. FEIGELSON, *Appl. Phys. Lett.* **19,** 237–240 (1971).
19. N. MENYUK, G. W. ISELER, AND A. MOORADIAN, *Appl. Phys. Lett.* **29,** 422–424 (1976).
20. J. L. DUNHAM, *Phys. Rev.* **41,** 721–731 (1932).
21. P. NIAY, P. BERNAGE, C. COQUANT, AND A. FAYT, *Canad. J. Phys.* **55,** 1829–1834 (1977).
22. A. G. MAKI AND F. J. LOVAS, *J. Mol. Spectrosc.* **98,** 146–153 (1983).
23. A. G. MAKI AND F. J. LOVAS, *J. Mol. Spectrosc.* **95,** 80–91 (1982).
24. A. G. MAKI, *J. Mol. Spectrosc.* **102,** 361–367 (1983).
25. P. BERNAGE AND P. NIAY, *J. Mol. Spectrosc.* **63,** 317–321 (1976).
26. A. G. MAKI AND F. J. LOVAS, private communication.
27. P. R. BUNKER, *J. Mol. Spectrosc.* **68,** 367–371 (1977).
28. J. K. G. WATSON, *J. Mol. Spectrosc.* **80,** 411–421 (1980).
29. A. H. WAPSTRA AND K. BOS, *At. Data Nucl. Data Tables* **19,** 175–297 (1977).
30. E. R. COHEN AND B. N. TAYLOR, *J. Phys. Chem. Ref. Data* **2,** 663–734 (1973).
31. J. P. BOUANICH, *J. Quant. Spectrosc. Radiat. Transfer* **19,** 381–386 (1978).
32. G. GUELACHVILI, D. DE VILLENEUVE, R. FARRENG, W. URBAN, AND J. VERGES, *J. Mol. Spectrosc.* **98,** 64–79 (1983).
33. R. M. DALE, M. HERMAN, J. W. C. JOHNS, A. R. W. MCKELLAR, S. NAGLER, AND, I. K. M. STRATHY, *Canad. J. Phys.* **57,** 677–686 (1979).